Magnetic Resonance in Medicine 65:457–462 (2011)

Post-Processing Correction of Magnetization Transfer Effects in FENSI Perfusion MRI Data

Olivier Reynaud and Luisa Ciobanu*

Magnetization transfer effects induced by repetitive saturation pulses employed in flow enhancement of signal intensity imaging sequences currently prevent quantitative, in vivo, cerebral perfusion studies. This study investigates the magnitude of these effects and introduces a post-processing correction protocol. The study shows that the magnetization transfer effect is consistent across individuals, which enables the derivation of a correction factor to be applied in post-acquisition. Our results, obtained for cerebral flux in white and gray matter in rodent brains, are in agreement with cerebral blood flow measurements previously reported in the literature. Magn Reson Med 65:457–462, 2011. © 2010 Wiley-Liss, Inc.

Key words: perfusion imaging; saturation pulses; magnetization transfer; flux; white matter

Measuring perfusion is useful in the diagnosis and treatment of a variety of conditions such as stroke (1), tumors (2), or chronic cerebrovascular diseases (3). Currently, there are two main methods for perfusion imaging in magnetic resonance imaging (MRI): dynamic susceptibility contrast (DSC-MRI) and arterial spin labeling (ASL).

In dynamic susceptibility contrast (DSC-MRI) (4,5) a bolus of paramagnetic tracer, such as gadolinium, is injected intravenously and a series of images are obtained as the tracer passes through the cerebral vasculature. By monitoring the tracer concentration time curves during the first passage, DSC provides information about different physiologic parameters such as cerebral blood volume, mean transit time, and cerebral blood flow (CBF) (6). Different imaging sequences allow access to large vessels and capillaries through the total cerebral blood volume or microvasculature pool (7,8). A precise quantification of CBF requires knowledge of the arterial input function, which can be obtained either by imaging small arteries or by proceeding to different imaging techniques such as positron emission tomography. Non-absolute quantification is often used, due to the low reliability of the arterial input function measurements (9,10). The main drawbacks of DSC are that it is invasive, the number of acquisitions per session is limited by the residual effect of the tracer (several hours), and it is complicated by the fact that the signal may depend not only on the tracer concentration but also on the tissue vascular composition.

Arterial spin labeling (ASL) is a completely noninvasive technique, which uses water as an endogenous contrast agent (11,12). In ASL the magnetization of blood is manipulated at a distance proximal to the slice of interest (this is referred to as tagging) and a tag image is acquired after a certain time required for the blood to travel to the imaging slice of interest. By performing a subtraction of the tag image from the control image one obtains an image of the blood that was delivered to the imaging slice. ASL allows for noninvasive quantification of CBF as perfusion or bulk delivery of blood to tissue. The standard ASL techniques suffer from low SNR from T_1 decay during the transit time.

Recently, a new MRI technique known as flow enhancement of signal intensity (FENSI) has been introduced (13). As with the ASL, the principle is to label the spins by manipulating the magnetization. The difference is that in the case of FENSI one saturates the magnetization in the slice of interest and then acquires the signal from a thicker slice, containing the saturated slice, as shown in Fig. 1a. The perfusion image is obtained by subtracting the tag image from a control image (no saturation). Compared with ASL, one expects FENSI to tag spins closer to the microvasculature as tagged spins moving fast in large vessels will exit the imaging slice during the experimental time. Similar to the microscopy DESIRE technique (14) from which FENSI originates, by repeating the saturation pulses for an extended amount of time one can obtain substantial signal enhancements, which allow thin-slice imaging (hundreds of microns). The signal enhancement comes only from the velocity component perpendicular to the tagging slice which also renders FENSI as directionally-sensitive.

Initially FENSI has been implemented as a functional Magnetic Resonance Imaging technique and was used to measure blood flow changes in response to a visual stimulus (13). A recent study reports FENSI experiments, which investigate the relationship between aging and spatial memory (15). Quantitative perfusion measurements using this technique are yet to be reported. As in all sequences involving repeated saturation pulses, the magnetization transfer (MT) effect can influence the signal intensity in the tag image and therefore hinder most quantitative studies. In ASL, where the tagging plane is located outside the saturation slice, one can compensate for magnetization transfer effects by acquiring the reference image with a "control" saturation pulse with the same frequency offset as the "tagging" pulse, but with opposite sign or by using a separate RF coil to do the

CEA, DSV, I2BM, NeuroSpin, LRMN, Gif sur Yvette, France.

Grant sponsor: French National Research Agency (ANR); Grant number: ANR-08-PCVI-0009-01.

*Correspondence to: Luisa Ciobanu, Ph.D., Neurospin, CEA Saclay, Gif sur Yvette, 91191, France. E-mail: luisa.ciobanu@cea.fr

Received 26 February 2010; revised 14 July 2010; accepted 10 August 2010.

DOI 10.1002/mrm.22625
Published online 22 September 2010 in Wiley Online Library (wileyonlinelibrary.com).

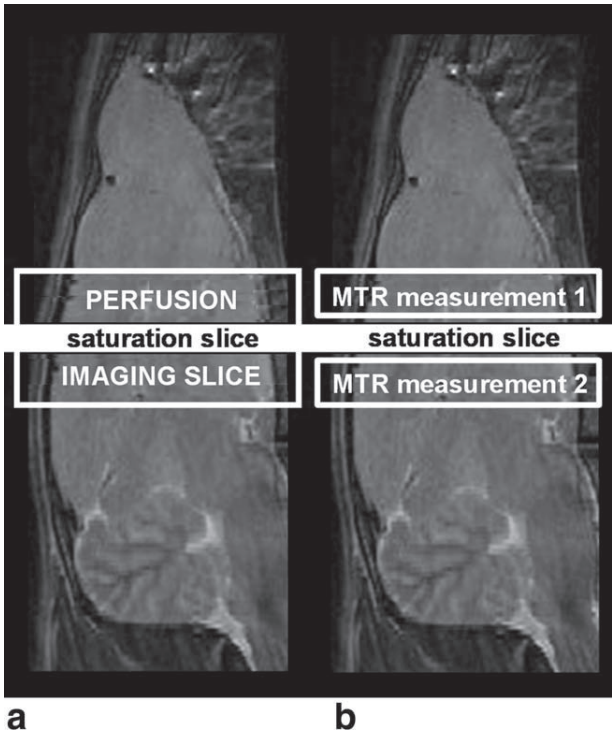

FIG. 1. Localization scan depicting a: the positions of the imaging and tag slices for FENSI protocol (imaging/saturation slice thickness = 3/0.3 mm) and b: the position of the tag slice and the region used to estimate the effect of magnetization transfer introduced by the saturation pulses (imaging/saturation slice thickness = 1/0.3 mm).

saturation. However, due to the position of the tag and imaging slice relative to each other, none of these two approaches can be used with FENSI. We have previously shown that the influence of the MT effects in DESIRE/FENSI based pulse sequences (16) is significant. In the absence of flow, experiments performed on agar gels showed that MT effects can lead to experimental signal enhancements twice as high as those theoretically calculated (due to diffusion). Because MT effects are both sample and pulse sequence dependent, these effects are difficult to predict and have so far prevented the application of FENSI to quantitative perfusion measurements (17).

In the current study, we measure the MT-induced effects for a specially-chosen set of experimental parameters and propose a post-processing protocol to correct for these effects and to obtain quantitative, in vivo, blood flux measurements using the FENSI technique. Our results from measuring the cerebral blood flux in white matter (WM) and gray matter (GM) are in agreement with the existing literature.

METHODS

Animal Experiments

Sprague-Dawley male rats with weights between 275 and 300 g were obtained from Janvier (Saint Isle, France). All experiments complied with French legislation and guidelines for animal research. For in vivo experiments, all animals were anesthetized with 2% isoflurane/air administered using a nose cone. The body temperature was maintained at 37°C using an MR compatible, feedback controlled air heater system. The respiration was continuously monitored. To estimate the MT in the absence of flow, the animals were euthanized 15 minute before the MTR measurements. We used one animal to study the influence of the total saturation duration (proportional to the number of pulses) on the amount of MT generated. Eight rats were used to estimate the possibility to quantify the effect of MT in WM and GM introduced by the saturation pulses and to generate MTR maps. We performed in vivo perfusion measurements on 10 animals.

MRI Acquisition

All scans were performed on a horizontal bore, 7T PharmaScan Bruker imaging system with a maximum gradient strength of 760 mT m^{-1}. A 3.6 cm ID quadrature RF coil was used for transmission and reception. Scout scans were acquired in three orthogonal directions to ensure similar localization in different animals. The FENSI-SE sequence used was a standard Spin Echo sequence (TE = 8.3 ms, TR = 3000 ms, resolution 200 × 200 × 3000 μm, FOV 30 × 30 mm; where TE is echo time, TR is pulse repetition time, and FOV is the field of view) preceded by a saturation module (150, 5 ms long 90° sinc shaped pulses, which saturate a 300 μm-thick slice in the center of the 3 mm imaging slice (Fig. 1a, total saturation duration 1500 ms). To obtain maps of the magnetization transfer ratio the pulse sequence was slightly modified to tag a 300 μm thick slice 1 mm away (to avoid direct saturation effects) from the imaging slice, chosen to be 1 mm thick. We performed two sets of MTR measurements, corresponding to two different positions of the tagging plane with respect to the imaging plane (Fig. 1b): above (MTR measurement 1) and below (MTR measurement 2). Two scans are required to calculate MTR in WM and GM, with and without saturation ("tag" and "reference"), the acquisition times remaining constant. For perfusion measurements each data set consisted of three images: a "control" image: 3 mm thick slice with no saturation, a "tag" image: 3 mm thick slice with saturation, and a "reference" image: 0.4 mm thick slice (effective tagging thickness) used to calibrate for static tissue. Segmentation of WM and GM regions was performed using a T_2-weighted FSE sequence (TE = 60 ms, TR = 3000 ms, NA = 4, Rare Factor 8, FOV 30 × 30 mm^2).

The effective slice profile generated by the FENSI module was experimentally measured using a water phantom (to avoid magnetization transfer and flow effects). We used the FENSI-SE pulse sequence described above in which we oriented the imaging plane perpendicular to the tagging slice and we increased the resolution across the tagging slice to 31 μm (FOV = 0.8 mm; np = 256) for better accuracy. The tagging profile was obtained by subtracting the "tag" image from the "reference" image.

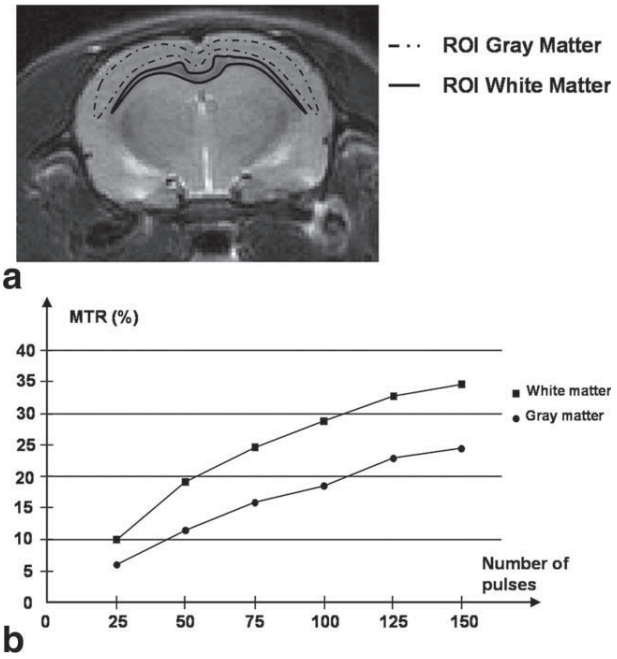

FIG. 2. a: Regions of interest used to calculate magnetization transfer ratios in WM and GM; the corresponding numbers of pixels are 156 and 500, respectively. b: Magnetization transfer ratio MTR as a function of the number of saturation pulses ($N = 25$ to 150) for WM and GM. Results were averaged over four slices.

Selection of Experimental Parameters

The choice of the parameters for a FENSI experiment depends on several factors. The signal enhancement obtained with the FENSI sequence depends on the velocity, the longitudinal relaxation time T_1, the tag duration and the imaging slice thickness. For an imaging slice thickness of 3 mm (1.5 mm on each side of the tag) and to sensitize our technique to microperfusion at the level of capillaries [average blood velocity of 1 mm s^{-1} (18)], we chose a tag duration of 1.5 s. This value ensures that spins labeled at the beginning of the tag do not leave the slice before imaging. Ideally, to maximize the signal enhancement one should continuously apply saturation pulses during the tag period. However, due to gradient duty cycle constraints, we separated our pulses by a 5 ms delay. Therefore, during our tag period we applied 150 saturation pulses of 5 ms length. Even though the duty cycle of the tag was only 50%, given our experimental parameters, effective tagging slice thickness 400 μm and interpulse delay of 5 ms we had very good tagging efficiency up to velocities of 8 cm s^{-1}. Therefore, we concluded that, within the microperfusion regime (average velocity 1 mm s^{-1}) the duty cycle employed did not affect the blood flux measurements.

Data Processing and Analysis

The MTR was quantified as a percentage of signal loss according to the following equation: MTR = 100* ($S_0 - S_{MT}$)/S_0 in which S_0 is the signal intensity for a particular region obtained without the saturation pulse and S_{MT} is the signal intensity for the same region with the saturation pulse. Pixel-by-pixel MTR maps were constructed. The mean MTR for the WM and GM was obtained by averaging the pixel values in the regions of interest selected for each slice. The regions of interest selected consisted of 500 ± 40 and 156 ± 30 voxels for GW and WM, respectively, as shown in Fig. 2a. We measured two MTR ratios for the two different experimental positions of the tagging plane, above (MTR_a) and below (MTR_b) the imaging slice and computed the average (MTR) for both the WM and GM regions of interest.

To obtain quantitative flow information based on FENSI images we corrected for the magnetization transfer effect present in the tag images. We performed this correction by using the following formula: $S_{COR} = S_{TAG}/(1 - MTR)$, where S_{TAG} is the uncorrected signal and MTR is the average value of the mean correction factors listed in Table 1: 37.5 and 26.5 for WM and GM, respectively. The intermediate parameter S_{COR} represents the signal intensity enhanced by flow after the MT correction. Brain microvasculature is characterized by calculating the flux ψ (mL min^{-1} cm^{-2}) defined by Eq. 1, where λ is the blood tissue partition coefficient [taken 0.9 and considered constant across the brain (19)], V_{TAG} the volume of one saturation voxel (mL), s_0 the static tissue signal ("reference") from the "tagging" plane (400 μm slice), and S_{CS} the cross-section of a voxel (in cm^2).

$$\phi = \left\{ \frac{S_0 - S_{COR}}{s_0} - 1 \right\} \cdot \lambda \cdot \frac{V_{tag}}{S_{cs}} \frac{60}{T_{sat}} \qquad [1]$$

RESULTS

Magnetization Transfer Effect

To quantify the magnetization transfer effect dependence on the number of the saturation pulses employed in the FENSI presaturation module we varied the number of saturation pulses from 25 to 150 and we calculated the

Table 1
Magnetization Transfer Ratio of White and Gray Matter Introduced by the FENSI Tag

MTRa map [%]	rat1	rat2	rat3	rat4	mean
White Matter[a]	41.0 ± 2.8	40.0 ± 3.2	41.1 ± 3.7	41.5 ± 3.5	40.9 ± 4.1
Gray Matter[a]	29.1 ± 3.0	28.6 ± 3.8	29.3 ± 3.3	29.1 ± 3.7	29.0 ± 3.4
White Matter[b]	33.9 ± 3.5	35.9 ± 3.5	35.4 ± 3.7	31.3 ± 3.2	34.1 ± 3.9
Gray Matter[b]	24.5 ± 3.2	24.9 ± 2.6	24.6 ± 3.2	21.9 ± 3.2	23.9 ± 3.3

The results are averaged over four different slices in four rats.
[a]Tag located above the imaging slice.
[b]Tag located below the imaging slice.

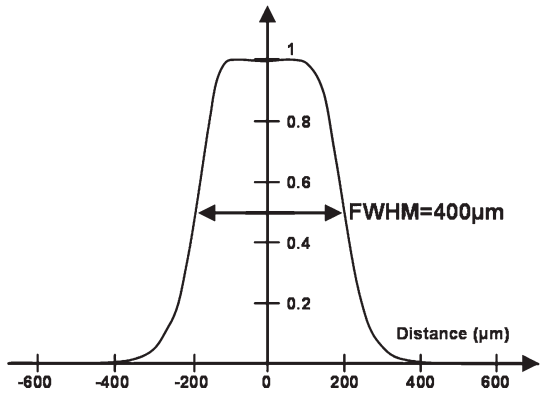

FIG. 3. FENSI tagging slice profile obtained by orienting the imaging plane perpendicular to the tag direction. The imaging resolution across the tag was 31 μm.

corresponding MTR as described in the methods section. Figure 2b presents plots of the magnetization transfer ratio, MTR versus the number of saturation pulses for WM and GM, averaged on four slices. One can see that, as expected, the magnetization transfer effect gets stronger as the number of pulses increases. For the parameters chosen in this study (150 pulses corresponding to 1500 ms saturation period) the magnetization transfer effect accounts for a decrease in signal intensity (increase in the FENSI enhancement) of up to 35% in WM and 24% in GM, respectively.

To estimate the variability of the MTR ratio across animals, we repeated the MTR measurements on four different animals (4 slices, using the same saturation period of 1500 ms). The results from these measurements are presented in Table 1. The decrease in signal due to the MT effect found in WM/GM was [34.1 ± 3.9%]/[23.9 ± 3.3%] when the tagging plane was placed below the imaging slice and [40.9 ± 4.1%]/[29.0 ± 3.4%] when the tagging plane was placed above. No significant difference was observed among the slices taken for the same individual or for different individuals. We thus concluded that the MT effect can be quantified once a particular set of experimental parameters was selected.

Effective Pulse Profile

The effective thickness of the tagging plane was measured as the full width at half maximum of the curve representing the saturation profile. We found an effective saturation thickness of ~400 μm (Fig. 3). The difference between the effective and the nominal saturation thicknesses, 400 versus 300 μm, is due to repetitive saturation. In a FENSI experiment, unless taken into account, this effect will lead to an apparent signal enhancement higher than the true flow enhancement, which will result in a higher blood flux. We corrected for this error by using a 400 μm slice thickness as reference for the static tissue of the tagging slice when computing the blood flux (s_0 in Eq. 1).

Perfusion Characterization After MT Correction

For ten animals, we obtained volumetric blood flux maps using the FENSI technique with and without the MT correction. The MT correction coefficients used are the mean values listed in Table 1. The WM and GM regions were segmented using the mask illustrated in Fig. 4a, and were found to agree well with the corresponding regions as seen in a typical MTR map (Fig. 4b). Given the strong effect of the magnetization transfer on the FENSI enhancement, as presented in the Magnetization transfer effect section, we expect that the uncorrected flux maps will not lead to accurate results. Indeed, the uncorrected maps (Fig. 5a) behave like MTR maps with hyperintense signals in the WM, blood flux value of 3.8 ± 0.4 mL min^{-1} cm^{-2}, compared with 3.1 ± 0.3 mL min^{-1} cm^{-2} in GM. However, the corrected maps (Fig. 5b) yield results, which agree with those previously reported in the literature. Specifically, we obtained blood flux values of 0.30 ± 0.35/0.74 ± 0.32 mL min^{-1} cm^{-2} in WM/GM, resulting in a ratio ψ_{WM}/ψ_{GM} of 0.4, in good agreement, as illustrated in Table 2, with the CBF ratio of obtained with other techniques such as ASL (20), DSC (4), positron emission tomography (4,21) or CT (22).

DISCUSSION AND CONCLUSIONS

The goal of this work was to investigate the magnetization transfer effect on FENSI cerebral perfusion images and to introduce a correction strategy. Our study shows

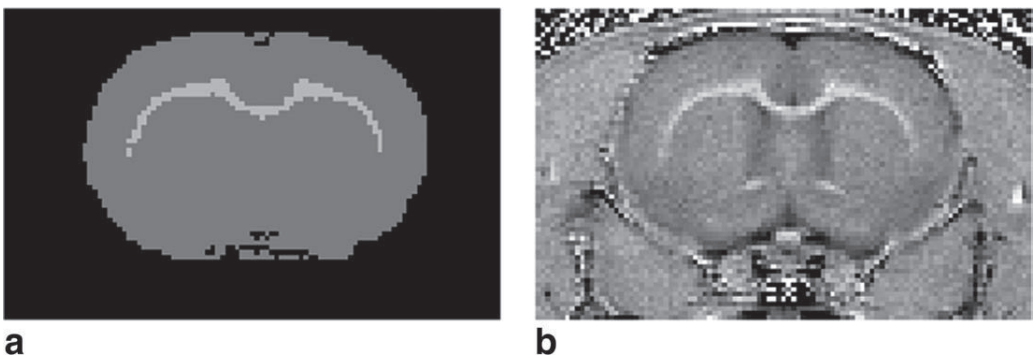

FIG. 4. a: MTR mask generated and used for post-processing. b: Ex vivo MTR map of a rat brain obtained with the FENSI-SE sequence (200 × 200 × 1000 μm) and 150, 5 ms long tag pulses.

that the effect of the magnetization transfer, for a particular set of experimental parameters, can be as high as 40% and 29% of the signal enhancement in WM and GM, respectively. We showed that this effect stays relatively constant across animals and across different brain regions and therefore can be measured and accounted for. Upon correction we obtain perfusion maps showing relative blood flow ratio WM/GM consistent with values reported in the literature. Direct comparison between the measurements made with FENSI and those made with other perfusion techniques such as ASL and DSC is complicated by the fact that ASL and DSC measure different aspects of blood flow; specifically, ASL and DSC measure bulk delivery of blood in mL/100 g of tissue/min while FENSI measures localized volumetric blood flux in units of mL min^{-1} cm^{-2}.

Even though the exchange rate between the macromolecular spins and the liquid pool is field independent the magnetization transfer ratio for a tissue increases as the field strength increases due to the increase in the longitudinal relaxation time (23). Therefore, for identical FENSI modules (the same number of pulses, power, shape, and duration) the MTR will be different at different field strengths. As a result, the correction factor cannot be transferred from one magnetic field strength to another and should be measured in each particular case.

In summary, we have attempted to tackle the magnetization transfer effects, a major obstacle to using the FENSI technique for brain perfusion measurements. We present here a protocol, which allows for MT correction in a post processing step and which can be used for quantitative CBF images. Another possible area of application is FENSI functional Magnetic Resonance Imaging where this protocol should improve the robustness of the acquired data through the removal of MT effects. In regards to the limitations of this approach, we emphasize that it should only be used in situations in which the magnetization transfer is not expected to change. It will therefore not be applicable to longitudinal studies in which the MTR ratio changes (e.g. angiogenesis); for these situations, other correction techniques are needed.

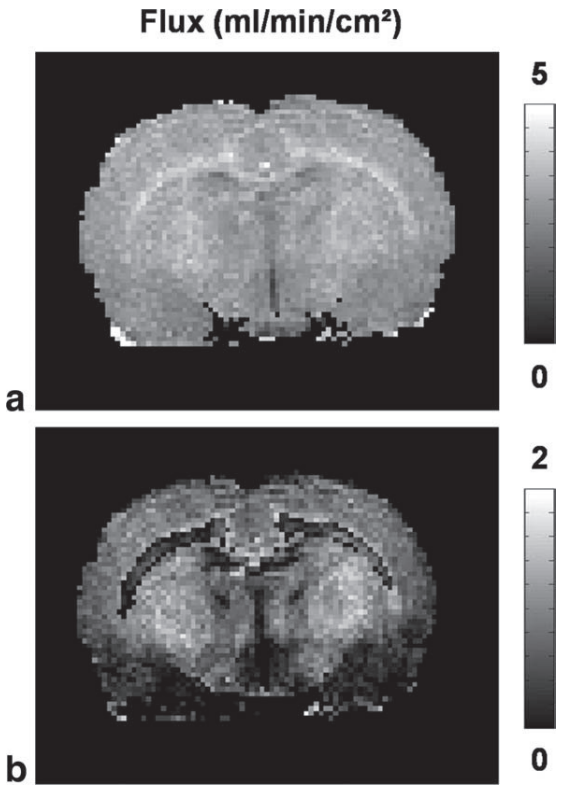

FIG. 5. Volumetric blood flux maps (mL min^{-1} cm^{-2}) a: without the MT correction and b: MT-corrected using the correction factors listed in Table 1.

Table 2
Comparison of the FENSI Flux Ratio (WM/GM) with the CBF Ratio Obtained with Other Methods

Method	PET	CT	DSC	ASL	FENSI
Flux or CBF ratio	0.45	0.30	0.37	0.33	0.41

ACKNOWLEDGMENTS

We acknowledge support from LRMN and LBI, Neurospin, CEA, Saclay. We also appreciate stimulating discussions with Dr. Brad Sutton from University of Illinois at Urbana-Champaign.

REFERENCES

1. Kloska SP, Wintermark M, Engelhorn T, Fiebach JB. Acute stroke magnetic resonance imaging: current status and future perspective. Neuroradiology 2010;52:189–201.
2. Pauls S, Mottaghy FM, Schmidt SA, Kruger S, Moller P, Brambs HJ, Wunderlich A. Evaluation of lung tumor perfusion by dynamic contrast-enhanced MRI. Magn Reson Imaging 2008;26:1334–1341.
3. Wolf RL, Detre JA. Clinical neuroimaging using arterial spin-labeled perfusion magnetic resonance Imaging. Neurotherapeutics 2007;4: 346–359.
4. Wittlich F, Kohno K, Mies G, Norris DG, Hoehnberlage M. Quantitative Measurement of Regional Blood-Flow with Gadolinium Diethylenetriaminepentaacetate Bolus Track Nmr Imaging in Cerebral Infarcts in Rats - Validation with the Iodo[C-14]Antipyrine Technique. Proc Natl Acad Sci U S A 1995;92:1846–1850.
5. Shin W, Horowitz S, Ragin A, Chen Y, Walker M, Carroll TJ. Quantitative cerebral perfusion using dynamic susceptibility contrast MRI: evaluation of reproductibility and age- and gender-dependence with fully automatic image processing algoritm. Magn Reson Med 2007; 58:1232–1241.
6. Weber MA, Risse F, Giesel FL, Schad LR, Kauczor HU, Essig M. Measurement of perfusion using the first-pass dynamic susceptibility-weighted contrast-enhanced (DSC) MRI in neurooncology. Physical basics and clinical applications. Radiologe 2005;45:618–632.
7. Fisel CR, Ackerman JL, Buxton RB, Garrido L, Belliveau JW, Rosen BR, Brady TJ. Mr Contrast due to microscopically heterogeneous magnetic-susceptibility - numerical simulations and applications to cerebral physiology. Magn Reson Med 1991;17:336–347.
8. Boxerman JL, Bandettini PA, Kwong KK, Baker JR, Davis TL, Rosen BR, Weisskoff RM. The intravascular contribution to Fmri signal change - Monte-Carlo modeling and diffusion-weighted studies in-vivo. Magn Reson Med 1995;34:4–10.
9. van der Weerd L, Thomas DL, Thornton JS, Lythgoe MF. MRI of animal models of brain disease. Methods Enzymol 2004;386:149–177.
10. Ashton E, Raunig D, Ng C, Kelcz F, McShane T, Evelhoch J. Scan-rescan variability in perfusion assessment of tumors in MRI using both model and data-derived arterial input functions. J Magn Reson Imaging 2008;28:791–796.
11. Detre JA, Leigh JS, Williams DS, Koretsky AP. Perfusion Imaging. Magn Reson Med 1992;23:37–45.

12. Williams DS, Detre JA, Leigh JS, Koretsky AP. Magnetic-resonance-imaging of perfusion using spin inversion of arterial water. Proc Natl Acad Sci U S A 1992;89:212–216.
13. Sutton BP, Ouyang C, Ching B, Ciobanu L. Functional imaging with FENSI: flow-enhanced signal intensity. Magn Reson Med 2007;58:396–401.
14. Ciobanu L, Webb AG, Pennington CH. Signal enhancement by diffusion: experimental observation of the "DESIRE" effect. J Magn Reson 2004;170:252–256.
15. Heo S, Prakash RS, Voss MW, Erickson KI, Ouyang C, Sutton BP, Kramer AF. Resting hippocampal blood flow, spatial memory and aging. Brain Res 2010;1315C:119–127.
16. Reynaud O, Le Bihan D, Webb A, Ciobanu L. Improved flow enhanced signal intensity (FENSI) perfusion imaging. International Conference on Magnetic Resonance Microscopy (ICMRM). West Yellowstone, Montana; 2009.
17. Reynaud O, Le Bihan D, Webb A, Ciobanu L. Magnetization transfer effect correction in DESIRE based pulse sequences. Euromar Magnetic Resonance Conference. Goteburg, Sweden; 2009.
18. Unekawa M, Tomita M, Tomita Y, Toriumi H, Miyakib K, Suzukia N. RBC velocities in single capillaries of mouse and rat brains are the same, despite 10-fold difference in body size. Brain Res 2010;1320: 69–73.
19. Herscovitch P, Raichle ME. What is the correct value for the brain–blood partition coefficient for water? J Cereb Blood Flow Metab 1985;5:65–69.
20. Yang YH. Perfusion MR imaging with pulsed arterial spin-labeling: basic principles and applications in functional brain imaging. Concepts Magn Reson 2002;14:347–357.
21. Vannucci R, Lyons D, Vasta F. Regional cerebral blood flow during hypoxia-ischemia in immature rats. Stroke 1988;19:245–250.
22. Beg S, Hansen-Schwartz J, Wikman P, Xu C-B, Edvinsson L. ERK1/2 inhibition attenuates cerebral blood flow reduction and abolishes ETB and 5-HT1B receptor upregulation after subarachnoid hemorrhage in rat. J Cereb Blood Flow Metab 2006;26:846–856.
23. Henkelman RM, Stanisz GJ, Graham SJ. Magnetization transfer in MRI: a review. NMR Biomed 2001;14:57–64.